

Erosivity and Performance of Nitrogen-Rich Propellants

Jonathan Lavoie,^[a] Catalin-Florin Petre,^[b] and Charles Dubois^{*[a]}

Abstract: Five propellant formulations were test fired both in a vented vessel and a closed vessel. Two formulations contained 35% weight of nitrogen-rich materials. The erosion by weight of the propellants ranged from 0.53 g to 1.31 g after two consecutive test firings of a given propellant. The addition of nitrogen-rich materials resulted in reduced erosion. Scanning electron microscope and energy dispersive X-ray spectroscopy revealed nitrogen in the ero-

sion pieces for one of the reference propellants (SB) and the two nitrogen-rich propellants. The two hottest propellants cause melting of the erosion pieces. The presence of nitrogen-rich materials has a tremendous impact on the burning rates with the burning rate increase at 100 MPa reaching up to 2.4 times that of the formulation used as the base for the nitrogen-rich propellants.

Keywords: Nitrogen-Rich · Erosion · Erosivity · Propellant · Burn Rate

1 Introduction

Gun erosion refers to the loss of steel in the bore of a gun barrel. This results in the wear of rifling and/or an increase in bore diameter. Since World War II, it is common knowledge for gun systems users/manufacturers that the erosion of gun barrels leads to two types of problems: (i) barrel replacement costs over the lifespan of fielded weapon systems, and (ii) reduced operational effectiveness due to variable gun performance and availability [1–5]. This is due to the effects of repeated firings on gun barrels, that even under normal firing conditions, are generally manifested in damage to the bore surface and a progressive increase of the bore diameter. The costs are not limited to the replacement of the barrel itself, but transportation of the gun barrel from its production facility to the location of the gun system is another contributing factor. These are non-negligible logistic costs that depend on distance and fuel prices.

There are three main approaches to mitigate gun barrel erosion: development of less erosive propellants, the use of coatings, treated barrel materials and liners, and erosion-reducing additives and lubricants. The most widely used approach is the use of protective coatings or surface treatments on the bore of the gun barrel. Normally, this is either done by depositing a thin layer of hard chromium inside the gun barrel or by nitriding (hardening) the interior of the barrel [1, 2]. These coatings/treatments are designed to mitigate all mechanisms of erosion, which are detailed below.

Multiple phenomena are responsible for gun barrel erosion, but they can usually be divided into three categories: mechanical action, heat transfer effects and changes in chemical composition. These phenomena are designated as mechanical, thermal and chemical erosion and they are tightly interdependent acting in concert to erode the barrels [3–5]. Mechanical erosion is caused by the friction from

a projectile (or its driving band) moving through a gun barrel and is out of the scope of this work.

Thermal erosion is caused by the morphological changes of the gun barrel steel, i.e. austenite and martensite phase transformation of steel and by the melting of the barrel material. Depending on the propellant used in the gun system and the rate of fire of the system, the steel temperature can get as high as 1800 K in a matter of milliseconds [3]. This is high enough to cause partial melting of the gun steel. The melting temperature of typical gun steel is 1723 K [1]. While temperatures of up to 1800 K can be attained, this is for very hot propellants and usually, the temperature of the gun barrel will be lower. For example, the barrel surface temperature for a Navy 5"/54 gun has been evaluated at 1450 K for XM-39 propellant which has a flame temperature of 2654 K [5].

Chemical erosion refers to the effects of chemical reactions occurring between the gun steel and the combustion gases generated by the propellant. The main combustion gases generated by a gun propellant are carbon monoxide (CO), carbon dioxide (CO₂), water (H₂O), hydrogen (H₂) and nitrogen (N₂). While other gaseous species are also formed, they are in small quantities and are usually lumped together or simply ignored in erosion modeling [4, 6, 7]. Each of these gases can react with gun steel to form various compounds. Some of these reactions are shown in equations 1 to 4 [8, 9].

[a] J. Lavoie, C. Dubois
*Chemical Engineering Department
École Polytechnique de Montréal
Montréal, H3C 3 A7 (Canada)*
**e-mail: charles.dubois@polymtl.ca*

[b] C.-F. Petre
*Defense Research & Development Canada Valcartier
Valcartier G1X 3 J5 (Canada)*



Iron carbide, formed due to the presence of CO and CO_2 , has a melting point around 1420 K, and other low melting point ferrous compounds are to be avoided to minimize erosion [1]. For the moment, there is no consensus on which combustion gas is the most erosive. Lawton has proposed a robust model with an erosion parameter based on the combustion gas composition of propellants commonly fielded in the United Kingdom, equation 5 [4].

$$\ln(A) = \ln(114) + 0.0207(f_{CO} - 3.3f_{CO_2} + 2.4f_{H_2} - 3.6f_{H_2O} - 0.5f_{N_2}) \quad (5)$$

Where “ f ” represents the volume percent fraction of the gas species in subscript and A is the erosivity in $m \cdot s^{-1}$. Jarlamaz et al. also proposed a propellant erosivity coefficient based on the gas composition, equation 6 [7].

$$\ln(A \cdot 10^3) = -0.27f_{CO_2} + 0.079f_{CO} - 0.14f_{H_2} + 0.35f_{H_2O} - 0.019f_{N_2} + f_R \quad (6)$$

Where “ f ” represents the fraction in % of the associated gas species, “ R ” standing for the remainder of the gas species and A is an erosion mass loss coefficient. Kimura proposed the following order for propellant combustion gases from the most chemically erosive to the least chemically erosive, equation 7 [9]. The difference in these models likely comes from the propellants and the experimental setup used given their empirical nature.

$$CO_2 > CO > H_2O > H_2 > 0 > N_2 \quad (7)$$

Kimura’s observation on CO_2 is also in agreement with erosion data from Conroy et al. [10]. Claims have also been made that high nitrogen content in the combustion gases could contribute to re-nitridation of the gun barrel and increase lifetime up to a factor of four [11]. The formation of iron nitride due to propellant combustion gas has been observed [1], but the propellants tested were limited to formulations made of conventional energetic materials. The research and modeling performed on the erosivity of combustion gases show a lack of consensus as to which gas is the most erosive. Despite the lack of consensus, there is agreement between various works that CO and H_2 increase the rate of gun barrel wear associated with the propellant. Comparatively, nitrogen gas is considered to have a lowering effect on gun wear.

The interdependence between the propellant and the thermal and chemical erosion becomes apparent. The pro-

pellant combustion is responsible for the heat generated in the gun. The composition of the combustion gases of a propellant depend on its molecular composition and its flame temperature. Finally, the reactions occurring between the combustion gases and the steel depend on the gas composition and temperature. As such, it stands to reason that adjustments to the flame temperature and combustion gases composition should have a direct impact on the erosivity of a propellant. While the amount of CO generated could be mitigated by a shift in the oxygen balance of the propellant, this would lead to a higher CO_2 and H_2O content while the nitrogen content remains constant. Given that nitrogen is not considered an erosive combustion gas, its generation should be prioritized. In fact, since it can be obtained from thermochemical calculations without experiments, the N_2/CO ratio has been used as an estimation of how erosive a propellant could be [12].

Based on the above, in order to design a low erosivity gun propellant, emphasis should be put on lowering the flame temperature and increasing nitrogen content in the combustion gases. This makes nitrogen-rich materials very interesting as they are mostly composed of nitrogen, often exceeding 80% by weight. It goes without saying that new propellants designed to have lower erosivity should also provide equal or better performance than the propellants they are designed to replace. The positive effects of nitrogen-rich materials on the burning rate of propellants have already been demonstrated by Mason et al. and Lavoie et al. [13, 14]. It was shown that in certain cases, despite the lower flame temperature, the experimental maximum pressure observed for nitrogen-rich propellants in a closed vessel was equivalent to that of formulations that did not incorporate nitrogen-rich materials, an indication that the same performance level is attainable [14]. This work is a follow up on the previous one [14] and focuses on the effects of two nitrogen-rich materials on the erosivity of gun propellants comparatively to standard formulations with matching impetus.

2 Results and Discussion

2.1 Vented Vessel Erosivity

An erosivity vented vessel allows observing the effects of the thermo-chemical erosion mechanisms, isolating their effects from the mechanical erosion mechanism. As such, two parameters are very important when conducting erosivity vented vessel experiments: the flame temperature and the composition of the combustion gases of the propellants investigated. Therefore, the propellant formulations from this study were all chosen based on the simulated thermochemical properties. Ideally, the burning rate of propellants should also be matched, or the geometry adapted to insure matching pressure-time profiles. However, it is currently not feasible to predict the burning rates of complex propellants

[15]. Insuring that the amount of energy contained in a propellant remains constant requires the design of complex propellants which is what motivated the use of thermochemical properties which can be predicted contrarily to burning rates.

Thermochemical data, calculated with Cheetah 7.0 is shown in Table 1. The nitrogen-rich formulations were designed to provide equivalent performance and thermochemical parameters to the reference propellants while increasing nitrogen content. For example, the N₂/CO ratio of MTB15 is four times greater than that of SB which should in theory help reduce the erosivity of the MTB15 propellant. In the case of MTB16, it provides the same amount of energy than JAM with increased nitrogen content and reduced flame temperature.

Table 1. Thermochemical properties of the propellants.

Propellant	F/ Jg ⁻¹	T/K	N ₂ / CO	CO/ CO ₂	P _{max, ad/} MPa	P _{max, exp/} MPa
SB	960	2602	0.20	9.75	246	220 ± 1
MTB15	987	2569	0.80	18.2	258	260 ± 1
JAM	1128	3305	0.30	3.96	282	265 ± 2
MTB16	1125	2951	0.77	21.5	293	246 ± 3
MTB17	1139	3229	0.29	4.55	286	266 ± 2

The maximum pressure observed experimentally in the vented vessel was 89% or more of the maximum adiabatic pressure (Table 1). This indicates that venting during combustion of the propellant and heat losses are minimal. Therefore, the composition of the combustion gases determined by the thermochemical calculations represents a good estimate of the combustion gases flowing through the erosion pieces.

The mass loss resulting from the erosivity of the propellants is shown in Figures 1 to 4. The measured erosion resulted from several phenomena: the chemical erosion resulting from reactions between combustion gases and steel, heat transfer including possible melting of the steel and friction from the flow of high pressure gases. The erosion on steel from a decommissioned M68 105 mm artillery gun was evaluated for the JAM propellant to compare with 4340 AISI steel. Mass loss for the gun steel was 1.58 g ± 0.15 g (one test firing) and 1.28 g (two consecutive test firings). Mass loss for the 4340 AISI steel was 1.52 g ± 0.20 g (single test firing per piece) and 1.31 ± 0.37 g (two consecutive firings per piece) which is the closest commercially available steel in term of composition to the M68 gun steel.

The absence of a rupture disc results in a different pressure history once an erosion piece is used more than once due to the change in diameter of the channel through which the combustion gases flow. To compare results between tests and propellants, the data was normalized according to equation 8. Equation 8 was chosen because a complete modeling of the transient flow of the gases was

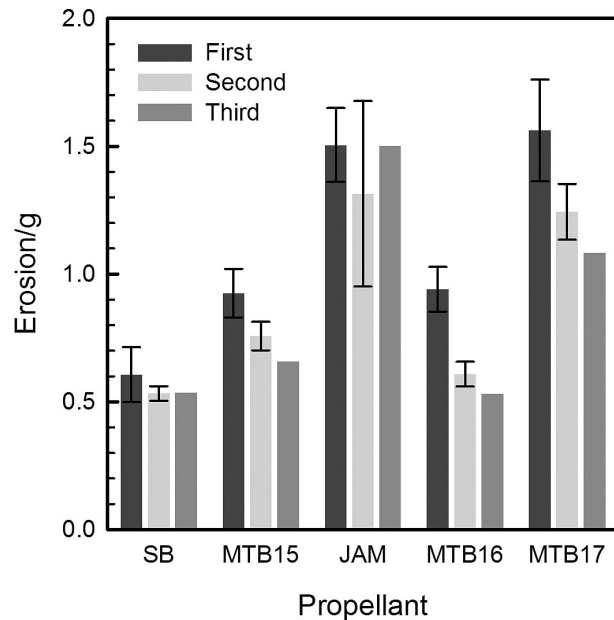


Figure 1. Erosion by weight loss between firings.

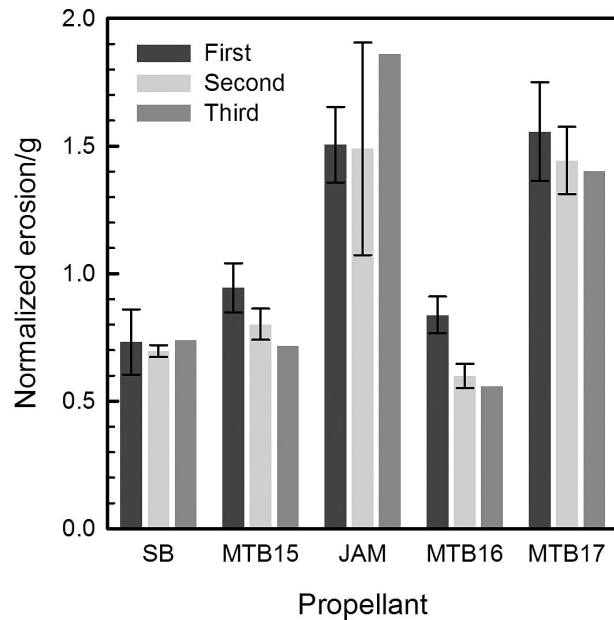


Figure 2. Normalized erosion by weight loss between firings.

not possible. The use of pressures avoided further mathematical treatment of the pressure-time data that could potentially induce errors or require additional assumptions. The principal limitation of this treatment is that significant differences in action time will not be entirely factored into the analysis. Normalized erosion will likely be overestimated for fast action times due to increased gas flow rates and underestimated for slow action times. This only affects SB and

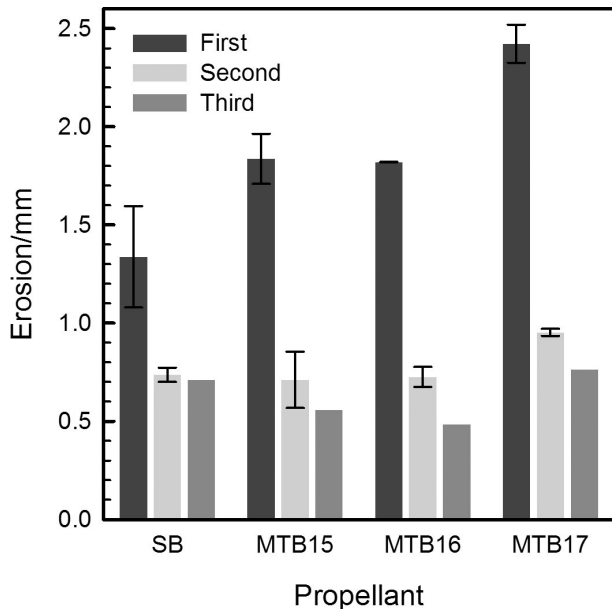


Figure 3. Erosion by diameter change between firings.

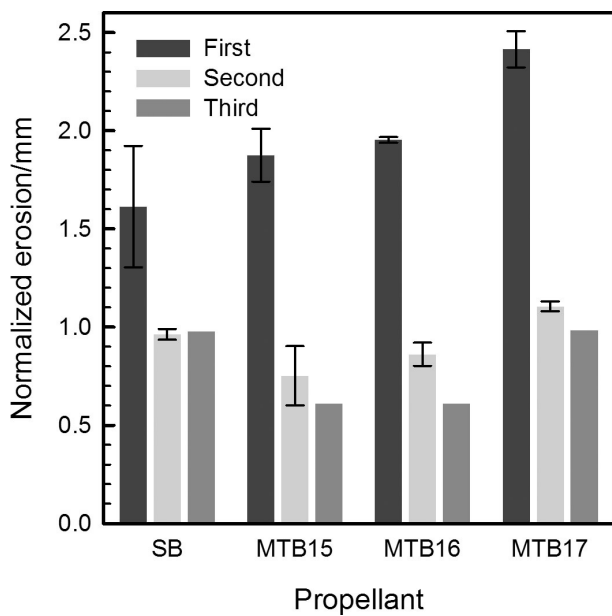


Figure 4. Normalized erosion by diameter change between firings.

MTB15, the other propellants remain unaffected. This will be elaborated on in the discussion of the erosivity results.

$$E_{\text{norm}} = E \left(\frac{P_m}{P_{\text{ref}}} \right)^{-1} \quad (8)$$

Where E_{norm} is the normalized erosion, E is the measured erosion, P_{max} is the maximum pressure for any given test and P_{ref} is a reference pressure. The reference pressure was chosen to be 265 MPa due to it being among the highest

pressure observed across all propellants. The erosion data was normalized to partially remove the effects of friction from high velocity gas flow compared to flame temperature and gas composition on the data. Higher pressure gas will have higher erosion due to higher velocity gas flow. This approach was verified using the results of JAM fired at respectively 0.1 g cm^{-3} and 0.2 g cm^{-3} which resulted in comparable normalized erosion. A total of three erosion pieces were tested per propellant. One piece was subjected to three consecutive firings, another to two and the last piece was subjected to a single firing. This explains the lack of error bars on the data for three firings as the results are for a single test piece. The pieces were weighed between each test firing. It was decided to measure the diameter of the erosion test pieces after most of the JAM propellant had been tested which is the reason why it is excluded from the thickness erosion results.

Figures 1 to 4 show the erosion by mass loss between consecutive firings and by the change in diameter between consecutive firings. Both values were measured as the change in mass loss will be influenced by changes in the steel composition due to gas species reacting with the steel.

It is important to note that some changes in mass of the erosion pieces will be due to the changes in steel composition. However, the thickness of the chemically affected layer of steel is quite small, evaluated to $\sim 20 \mu\text{m}$ after 10 shots in a vented vessel [4]. As a result, the impact on the change in mass will be low compared to the loss of material due to erosion. Figure 2 shows that JAM and MTB17 are the two most erosive propellants tested. This was expected based on composition of the combustion gases and adiabatic flame temperature. SB is a generally considered a *cold* propellant and as such was expected to show lower erosivity. Even when using normalized data, MTB15 proved to be more erosive than SB, mainly because it has a burning rate that is roughly four times faster than that of SB. The burning rates will be discussed in the section on performance. The approach used to normalize the erosivity is solely based on the maximum pressure and as a result, does not account for the flow pattern history of the combustion gases. It was found that MTB15 exhibited significantly faster pressure rise in the vented vessel than all the other propellants (Figure 5).

It is expected that this behavior will significantly increase the erosion due to the mechanical action of the gas flow. The SEM micrograph of the piece subjected to three firings of MTB15 showed significant cracking in the flow direction at a higher degree than any of the other propellants (this will be elaborated on the next section). This is indicative of a high mechanical stress which likely amplified the erosion significantly and would explain the higher erosivity comparatively to the SB propellant. The higher erosion for the first test compared to pieces that were subjected to two or three tests supports the idea of strong flow erosion effects for MTB15. The change in diameter for

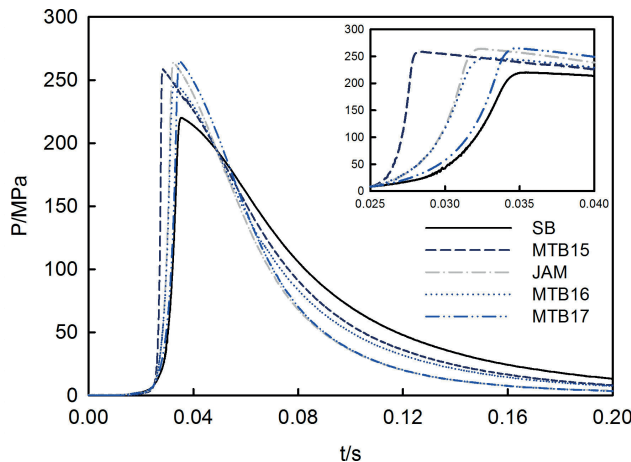


Figure 5. Pressurization of the vented vessel during a first test firing.

MTB15 is similar to the change in diameter for SB on pieces subjected to two or three test firings. The change in the shape of the channel of the steel pieces compared to other pieces where no melting occurred also supports strong gas flow effects (Figure 6).

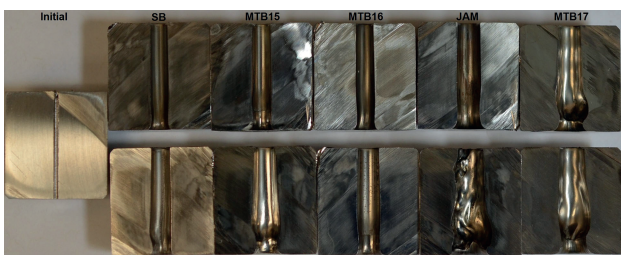


Figure 6. Cut erosion test pieces after two (top) and three (bottom) test firings.

Interestingly, MTB16 was the least erosive propellant despite a temperature of 2951 K, higher than that of MTB15 (2569 K) and SB (2602 K). This can be attributed to the higher nitrogen content of the combustion gases. The photos sectioned erosion pieces for MTB16 also show no evidence of melting and uniform erosion along the whole channel (Figure 6).

JAM and MTB17 are the two propellants that show evidence of the erosion pieces melting. For JAM, the melting occurred only after three test firings and was quite pronounced. For MTB17, melting was observed after two firings, but is less pronounced than it was for JAM. The high normalized erosion of JAM after three tests agrees well with the observed melting.

A behavior that was observed for all propellants was that the erosion for the first test was much higher than for any subsequent tests. This results from the small initial diameter of the erosion pieces which is small enough to ex-

perience a large amount of mechanical erosion from the flow of combustion gases. The effects of gas flow are also evidenced by the formation of a curvature at the entry point of every erosion piece as easily evidenced by Figure 6.

Changes in erosion for three consecutive test firings are shown in Table 2 relative to the erosion of SB, JAM and MTB17, the three reference propellants. Table 2 shows that from a mass loss standpoint, MTB16 is the least erosive propellant after three consecutive firings and that MTB15 remains less erosive than any of the reference propellant. The changes in diameter show that both propellants show similar erosivity between the second and third test firings. The likeliest explanation for the discrepancy between the changes in mass and diameter is that the reaction of the combustion gases with the steel results in the formation of ferrous compounds that have an influence on the final mass of the erosion piece. The pieces subjected to three consecutive firings were weighed after being thoroughly washed to ensure that combustion residue had no influence on the calculated data. The amount of combustion residue present in the channel of the erosion pieces was also found to have a negligible influence on the change in weight before and after washing the erosion pieces for all tests (two orders of magnitude lower).

Table 2. Normalized erosion relative to the reference propellant formulations.

	SB	JAM	MTB17
MTB15 (weight)	0.97	0.39	0.51
MTB16 (weight)	0.76	0.30	0.40
MTB15 (diameter)	0.62	N/A	0.62
MTB16 (diameter)	0.62	N/A	0.62

It is also interesting to note that the molar concentration of hydrogen in the propellants was the highest for the two nitrogen-rich propellants at 22% compared to 19% for SB, 12% for JAM and 13% for MTB17. Hydrogen has been postulated to promote heat transfer and often results in higher erosion by weight loss at lower flame temperatures [9]. A linear relationship between the logarithm of the erosion and the square root of the ratio of the flame temperature to the molecular weight of the combustion gases was previously observed, illustrating the influence of hydrogen content on increased heat transfer which results in higher erosion [9]. The normalized erosion of the three conventional propellants follows this trend well across all tests for any number of firings on the same erosion piece. The exception was the JAM test where important melting and higher erosion occurred. MTB15 appears to follow the same trend to some degree, however MTB16 is a clear divergence from this trend with a much lower erosivity at the same $\sqrt{(T/M_w)}$ to the other propellants (Figure 7).

As previously discussed, MTB15 firings resulted in pressurization of the vented vessel roughly three times as fast

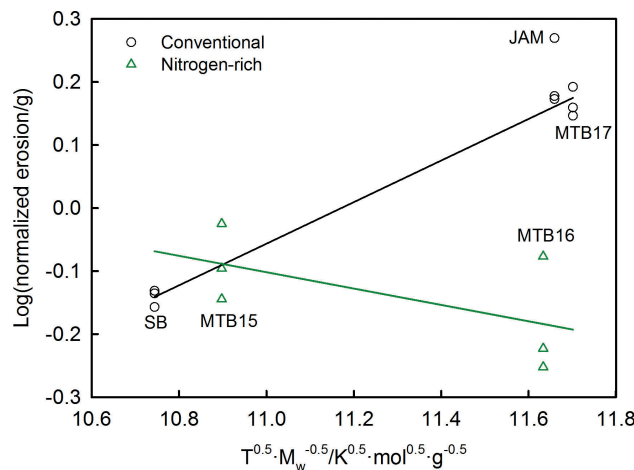


Figure 7. Effects of flame temperature and gas molecular weight on erosion.

as SB and twice as fast as the other propellants. The normalization of the erosion data is therefore likely to have less of an impact on MTB15 and the effects of the gas flow will remain higher compared to the other propellants. The chemical and thermal erosion effects are expected to be lower than the ones presented in Figure 7. Another hypothesis that could explain, at least partially, the lower erosion as a function of $\sqrt{T/M_w}$ is the improved heat transfer that results in two opposing effects: reactions of steel with carbon and oxygen which increase erosion competing with nitriding of the steel which decreases erosion. Depending on the quantity of nitrogen in the combustion gases, nitriding of steel should be the dominant reaction. This could lead to hot propellants with low erosivity to a certain extent. Propellants hot enough to cause bore temperatures of 1700 K or more would still result in melting of gun steel regardless of the nitrogen content. More experimental work is needed to confirm whether this would be the case, but the results of this study highlight this possibility.

2.2 Scanning Electron Microscopy

Carbon contamination from sample handling and organic compounds present in the laboratory is difficult to avoid completely. A composition analysis on the non-reacted steel outside of the channel where gas flow occurred gave 2% to 4% weight carbon which gives a qualitative estimate of initial carbon contamination. Therefore, any carbon content not significantly different from those values was not considered as a possible indicator of the presence of carbide species in the analysis. Cementite (Fe_3C) is the expected carbide species to be encountered. This was observed previously as one of the principal mechanisms of gun barrel erosion [1, 2, 5, 8, 9] and given both the composition of the 4340 steel and the combustion gases is the carbide most

likely to occur from reactions between combustion gases and steel. Reaction products resulting in the detection of additional carbon in the steel are collectively referred to as carbides in the discussion.

Unexpected traces of contamination were found by the EDS detector during the SEM experiments. This was puzzling at first and made interpreting the results of the EDS detector more difficult. Figure 8 shows examples of the contamination observed. The top image shows droplets from what was identified to be weld contamination on the piece subjected to 3 test firings of SB. These droplets were identified to be either mainly tin (50+ % weight) or a lead-tin alloy, 3:4 weight ratio. The droplets were thin enough for some iron to be detected by the EDS detector. Iron, carbon, oxygen and other elements composed a minority of what was detected. The middle image taken from the piece subjected to 3 tests with MTB15 is splatter from lead at 21% weight, the layer was thin enough to detect 59% weight of iron along with some carbon (9%) and oxygen (8%). The bottom image shows splatter composed mainly of copper. Part of the carbon is expected to come from combustion residue rather than having reacted with the steel. Potassium, sulfur, copper or a combination of these elements were always present with the contamination. This contamination is expected to come from the igniter where copper, black powder and the electric match charge and support is the likeliest source for the contamination.

Any location where significant amounts of contamination were detected were not factored into the analysis and discussion of the effects of the combustion gases on the erosion pieces that follows.

The erosion mechanisms of the two hottest propellants (JAM and MTB17) appear to differ significantly from the other three. Table 3 shows the atomic content of iron, carbon, oxygen and nitrogen found in the erosion pieces after two test firings. For comparison, a non-tested piece parts of the segmented erosion pieces not exposed to the propellant gases is shown.

Table 3. Atomic composition after two test firings.

	Fe/atomic %	C/atomic %	O/atomic %	N/atomic %
AISI 4340 steel	94	2	0	0
Non-exposed steel ^{a)}	82–84	10–14	0–6	0
SB	57–58	25–30	10–13	0
MTB15	62–70	20–25	4–9	2–5 (at 5 kV)
JAM	62–70	22–27	5–9	0
MTB16	55–64	24–29	7–15	3–7
MTB17	68–78	14–20	3–5	0

a) Part of the Erosion Piece not in Contact with the Combustion Gases

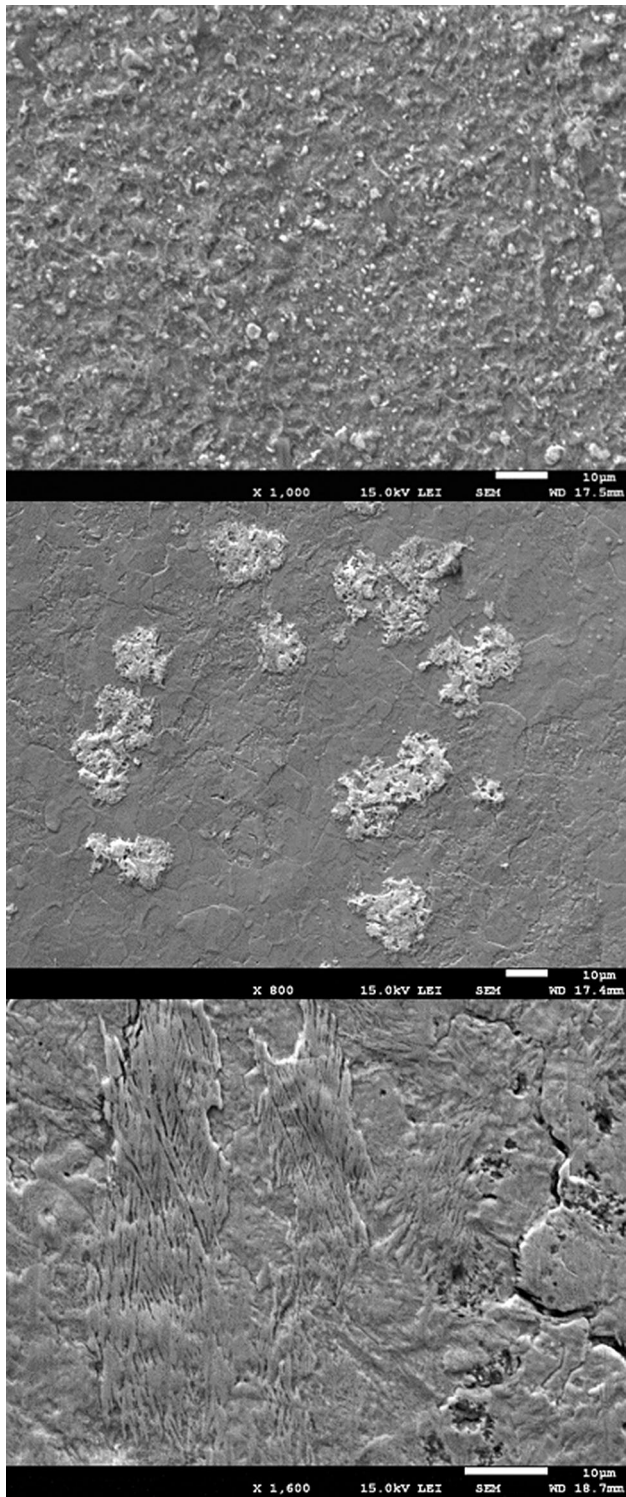


Figure 8. Contamination from the ignition system: lead and tin droplets (top), lead and tin splatter (middle), and copper splatter (bottom).

After two test firings, what is believed to be chemical etching appears on the test pieces subjected to SB, MTB15

and MTB16. Figures 9 to 11 show images of erosion pieces subjected to two test firings of propellants SB, MTB15 and MTB16 at low and high magnification. The “needle” like structures formed by the reaction with the combustion gases are visible for all three propellants, but are much more pronounced for SB than the other two propellants. Sites free of visible igniter contamination on the piece in contact with the combustion gases of SB exhibited atomic oxygen content of around 10%–13%, higher carbon content (25%–30%) with 57%–58% iron. The balance was a very small amount of igniter contamination and nickel which is present in AISI 4340 steel. This indicates it is more likely that SB results in the formation carbides than oxides. The flame temperature of SB is low enough that any formed Fe_3C is not expected to melt. Small amounts of nitrogen were sometimes also detected. Composition analysis of pieces in contact with MTB15 after two firings showed no distinct oxide layers and the chemical attack appears to be less important than for SB. Any layer found on the erosion pieces was due to igniter contamination. Atomic varied between 62%–70% Fe, 20%–25% C and 4%–9% O. This is indicative of some amount of carbides with only a very small amount of oxide, given that manganese, chromium, nickel and the other components of 4340 AISI steel were usually detected on these sections, it is expected that not all steel was converted to carbides and that some of the carbon content is combustion residue and organic compounds. At 15 kV, a nitrogen peak was observed, but the deconvolution algorithm used by the software resulted in a negative peak area. Scans taken at 5 kV yielded better results and puts the nitrogen atomic content between 2% to 5% in areas where no igniter contamination was observed. These proportions are not exact as nitrogen cannot be quantified accurately using SEM-EDS, but the apparition of nitrogen is likely to indicate the formation of nitride species. The electrons can penetrate approximately 1 micron at 15 kV and only 0.16 microns at 5 kV. Interestingly, where layers of metal splatter from the igniter were detected, higher nitrogen content was also observed. This is either due to unburnt propellant buried under the contamination or other nitrided species like Cu_3N .

MTB16 shows similar results to MTB15 with an atomic composition in areas free of contamination of 55%–64% Fe, 24%–29% C, 7%–15% O and 3%–7% N. In this case, the nitrogen could be detected even at 15 kV. The preferred hypothesis for the higher oxygen and carbon content is the flame temperature of MTB16 favoring the reaction between the combustion gases and the steel. This would also favor higher nitrogen content which as observed. This higher nitrogen content is line with the lower relative erosivity of MTB16 compared to all the other propellants. The chemical attack of the combustion gases which in this case is evidenced by the change to a needle like structure was also lesser for MTB16 compared to SB. The overall carbon content is also lower for the nitrogen-rich propellants than it is for SB. The handling of all samples was kept identical, there-

fore, any change in atomic content is expected to be a result of the effect of the propellant composition.

Also visible on Figure 9 are the impact from impinging particles, contamination from the igniter and stress cracks in the flow direction from the gas pressure. The fact that cracks do not follow the grain of the steel is attributed to the stress imparted by the high pressure during the tests rather than thermal expansion and contraction.

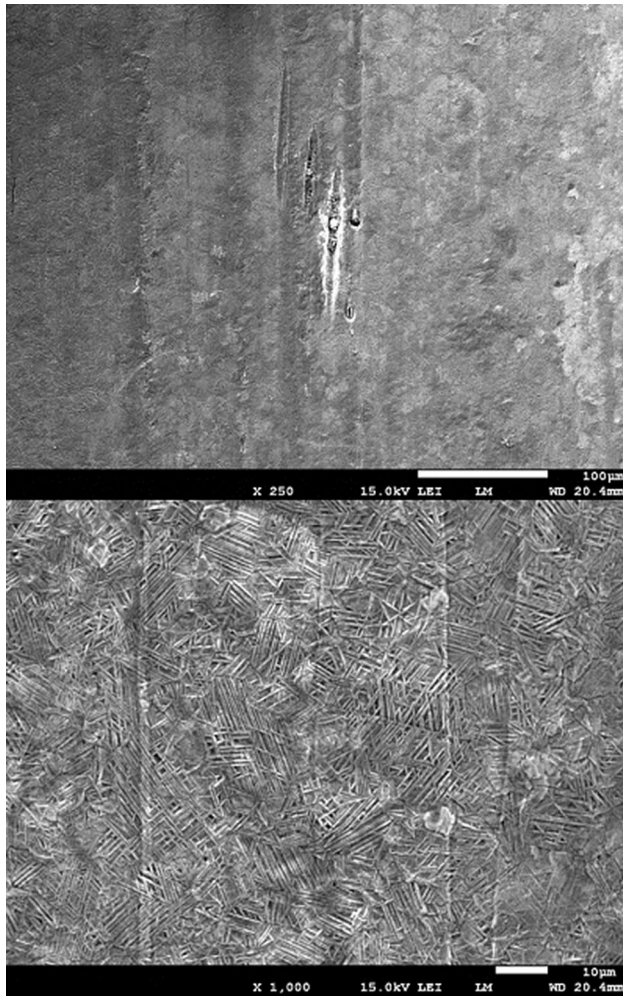


Figure 9. Erosion pieces after two test firings of propellant SB: low magnification with impinging particles impact (top) and high magnification with needle-like structure (bottom).

Test pieces subjected to JAM and MTB17 firings exhibited significant cracking as evidenced Figures 12 and 13. This cracking follows the grain of the steel and is attributable to rapid heating and cooling of the material which results in rapid thermal expansion and contraction of the material. The resulting stress causes the formation of cracks along the grain of the steel. The higher magnification images for MTB17 also easily show that the temperature of the steel was high enough for a change to austenite and

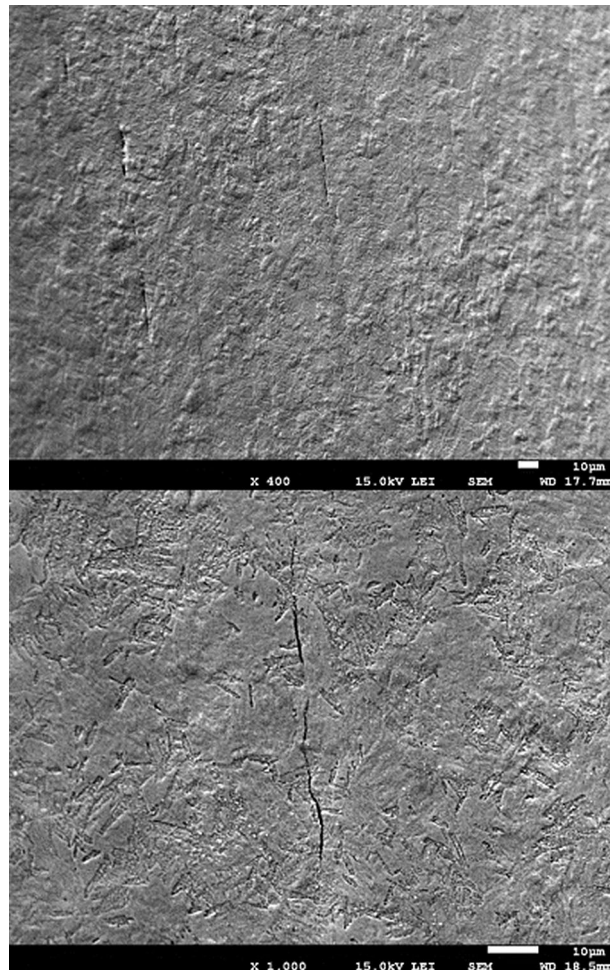


Figure 10. Erosion pieces after two test firings of propellant MTB15: low magnification with stress cracking (top) and high magnification with stress cracking (bottom).

subsequently martensite upon cooling for which the needle like structure is clearly shown in Figure 13. This was also considered as a confirmation that the needle like structures visible in Figures 10 to 11 were the result of chemical reactions rather than thermal shock. These phase transitions are accompanied with changed in density and cause additional stress in the material. The change in chemical also results in density changes. The cracking suggests that the erosion mechanism for the two hotter and more erosive propellants is clearly different than for the other three propellants.

Atomic carbon content relative to iron varied between 0.25 and 0.5, part of this carbon content is attributable to small portions of carbides, combustion residue trapped in the oxide, especially when cracks are present and contamination from organics which despite best efforts could not be entirely avoided and make up the remainder of the carbon content. Any pits or cracks would limit the effectiveness of washing the erosion pieces and leave combustion

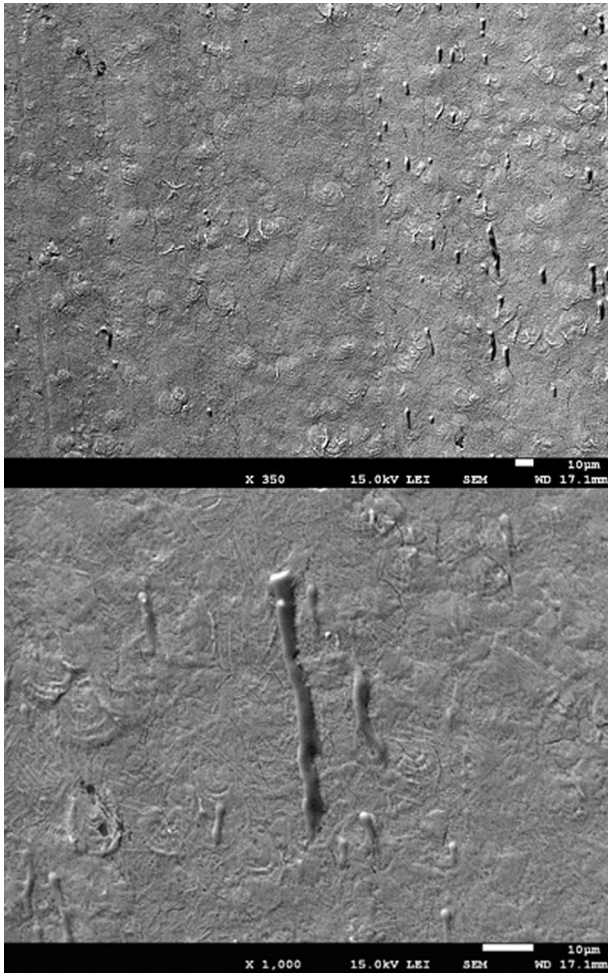


Figure 11. Erosion pieces after two test firings of propellant MTB16: low magnification (top) and high magnification with some needle-like structures (bottom). Also visible, contamination splatter from the ignition system.

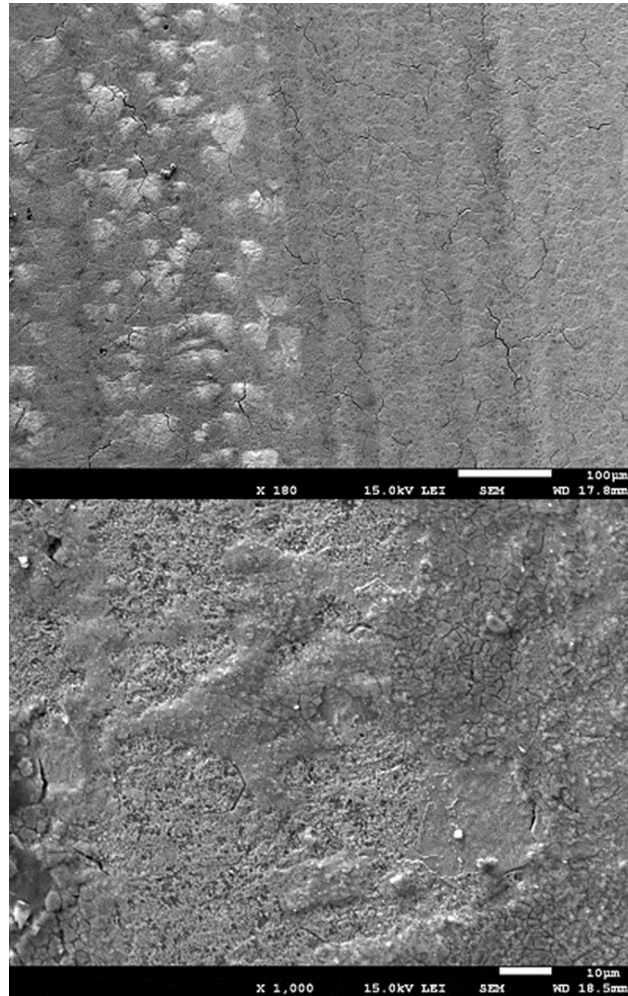


Figure 12. Erosion pieces after two test firings of propellant JAM at low and high magnifications with thermal stress cracking.

residue with high carbon content. This was observed across all samples where any composition analysis locations that could easily trap combustion residue resulted in higher carbon content. Analysis on what appeared to be steel with no igniter contamination or oxide layers yielded an atomic composition of 62%–70% Fe, 22%–27% C and 5%–9% O for JAM and 68%–78% Fe, 14%–20% C and 3%–5% O. This indicates that MTB17 results in lower F_3C content than JAM. This is also consistent with the observed pronounced melting of the erosion piece exposed to three firings of JAM (Figure 6) where high carbide content explains the significant melting of the material. What appears as melt was also observed for MTB17, but on a much smaller scale. Smaller amounts of localized melting which could partially solidify before exiting the erosion piece would explain the overall lower carbon content after two firings as formed iron carbide would melt and be wiped by the gas stream. This is consistent with the observed area where there is a

widening of the channel for MTB17 which was not observed for the other propellants including JAM. The irregularity of the widening also points to partial melting of the material instead of a purely flow induced phenomena as would be the case for the other propellants after two test firings.

A summary of the atomic composition where morphological changes were not significant for test pieces subjected to three consecutive test firings for all propellants is shown in Table 4.

After three test firings, formation of carbides, most likely Fe_3C , accompanied by a distinct change in morphology was also observed for SB. The atomic composition was evaluated at 67% Fe and 27% C. Carbon content is easily influenced by organic contamination that is present in the air and could be deposited during handling of the samples. Combustion residue is also a potential source of contamination although, a layer of residue was not observed with the SEM. The change in morphology as evidenced in Figure 13 also supports a change in chemical composition.

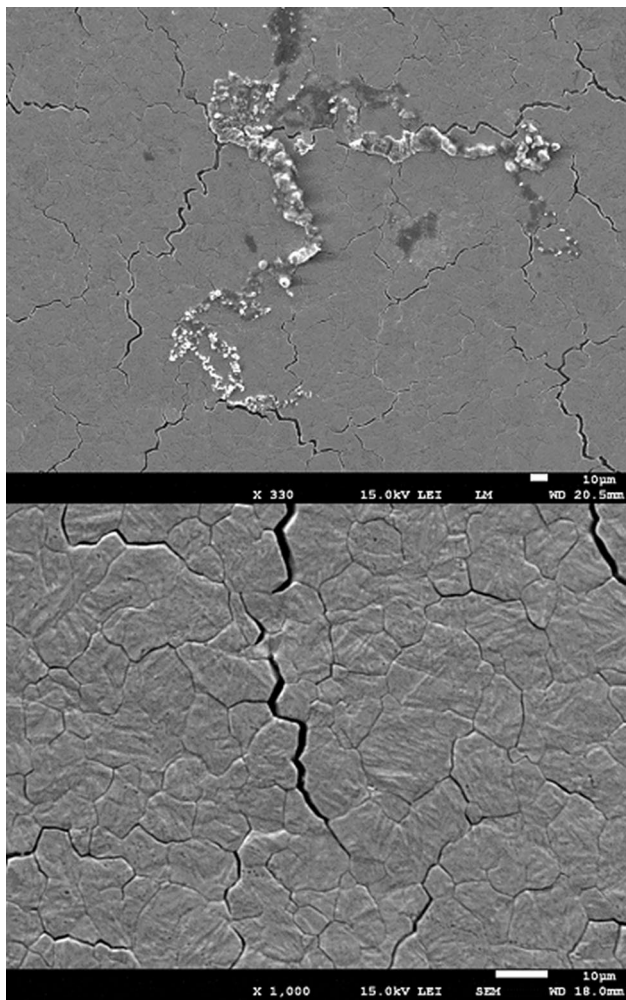


Figure 13. Erosion pieces after two test firings of propellant MTB17: low magnification with thermal stress cracking (top) and high magnification with stress cracking and martensite formation due to thermal shock (bottom).

Table 4. Atomic composition after three test firings.

	Fe/atomic %	C/atomic %	O/atomic %	N/atomic %
Non-exposed steel	82–84	10–14	0–6	0
SB	69	21	2	0–5
MTB15	82–87	11–16	0	0
JAM	34–40	11–20	38–44	0
MTB16	66–68	22–29	0–11	4 (5 kV)
MTB17	29–34	14–21	49–52	0

In locations where no morphological changes were observed for three SB firings, the iron content was higher than the piece after two firings at 69% and the overall carbon and oxygen content were lower, 21% and 2% respectively. This would be indicative of the reacted layer being removed and that reaction of the steel with the combustion gases

takes place over more than one test firing until it reaches a point where a significant portion of the reacted material is ablated. The carbides also exhibit signs of stress cracking which was not observed in the bulk of the material after two firings. In the case of MTB15 after three test firings, the atomic composition of the piece was 82%–87% iron, 11%–16% carbon with no traces of oxygen, the other elements present in 4340 AISI steel, even those not often detected in areas where high carbon content was observed like molybdenum were detected in this case. The exposed layer, Figure 6, was observed to a much lower degree than after two firings, cracks in the flow direction were also observed throughout the surface of the erosion piece (Figure 14). No nitrogen was detected. The formation of nitrides after two firings would help form a barrier to limit the reactions between CO and CO₂ and the steel. The reacted hard layer however is ablated by the very high velocity gas stream resulting from the high burning rate of MTB15 in the subsequent (and third) test exposing what is essentially virgin steel. After three test firings, content for the piece exposed to MTB16 was evaluated at 66%–68% Fe, 22%–29% C and 0%–11% O. The overall higher iron content and lower oxygen content seem to indicate that the presence of nitrogen formed nitrides that partially protected unreacted steel. Nitrogen was detected at 15 kV, but suffered from the same issues mentioned previously where the deconvolution algorithm gave it a negative peak area. At 5 kV, the atomic nitrogen content was evaluated at 4%. The presence of nitrogen indicates that the protective nitrides generated by the propellant during each shot which was not the case for MTB15. This agrees with the lower erosion of MTB16 compared to MTB15 and the other propellants.

A significant amount of oxygen was found on the erosion piece subjected to three tests with JAM. Atomic proportions of 34%–40% Fe, 38%–44% O and 11%–20% C were detected. This is consistent with a mixture of FeO, other oxides such as Fe₃O₄, likely some carbides and trapped combustion residues, FeO and Fe₃O₄ have previously been observed in erosion testing [9]. The oxide was visible with the naked eye for the piece exposed to JAM and the dark color is indicative of oxides different from Fe₂O₃. The oxide layers caused by MTB17 had a different atomic composition with 29%–34% iron, 49%–52% oxygen and 14%–21% carbon. The higher oxygen content is likely to result from a different proportion of oxide species than for JAM given the difference in gas composition and flame temperature. The oxide layers, shown in Figure 15, were cracked and partially ablated for both propellants. This is another good indication that cracking and subsequent ablation of the ferrous species by the gas flow plays a more important role in the erosion caused by JAM and MTB17 compared to the other three propellants. While the composition of individual elements could be measured using the EDS detector, it is difficult to identify the specific species of ferrous compounds present given that multiple species coexist together. However, the increase in carbon and oxygen content

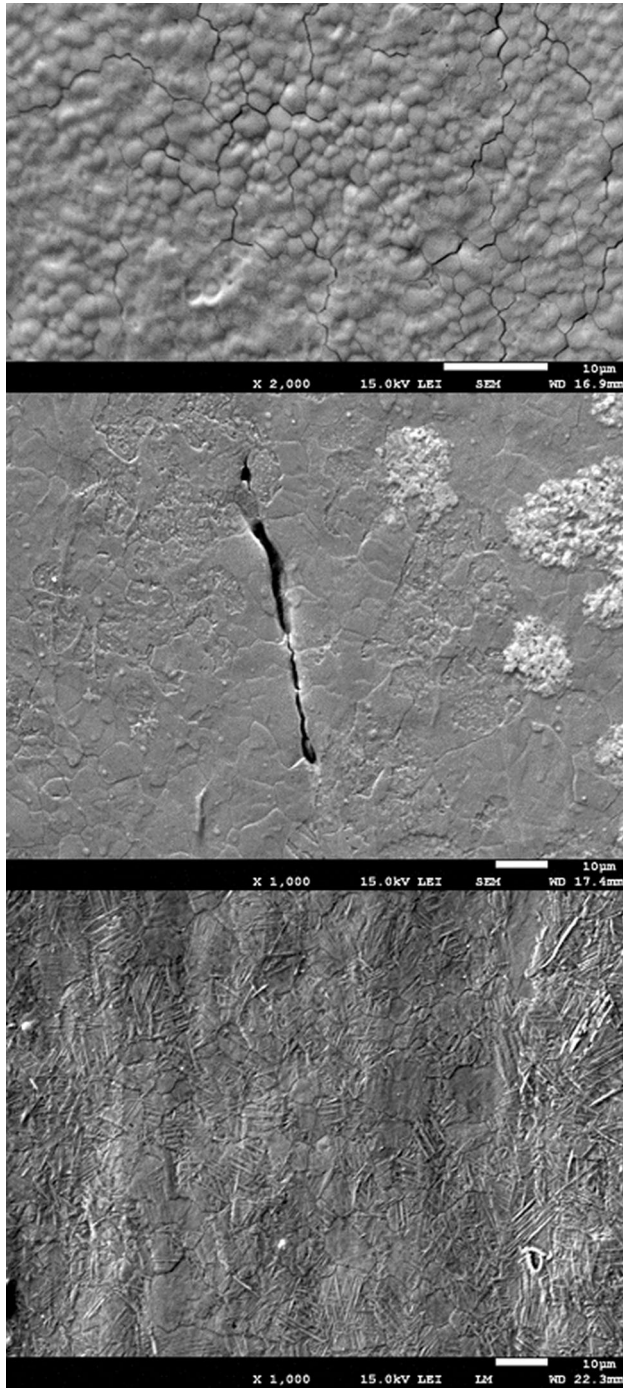


Figure 14. Following three tests: SB (top), MTB15 (middle), MTB16 (bottom).

confirm the formation of carbides and oxides. The presence of nitrogen on pieces tested with MTB15 and MTB16 is encouraging in validating the hypothesis that nitrogen-rich propellants form protective nitride species when used. These do not prevent the formation of carbides and oxides, but help in limiting the erosion resulting from the propellants nonetheless. X-ray diffraction analysis also confirmed

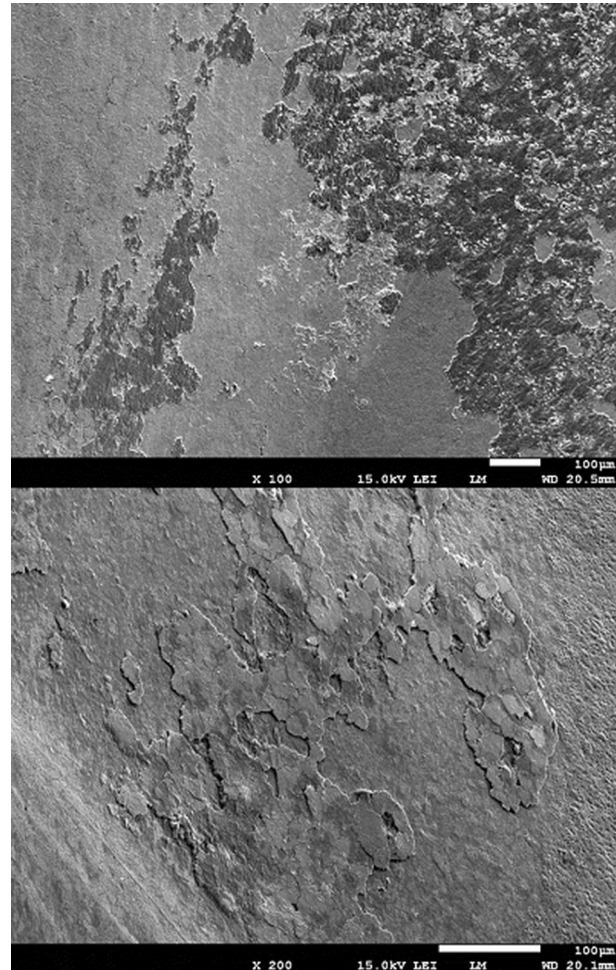


Figure 15. Following three tests: iron oxide from JAM (top) and MTB17 (bottom).

the presence of a cubic structure of iron nitride, especially on the MTB16 samples (data not shown). More tests will be performed in the future done to couple the SEM/EDS and XRD results. No iron nitride was observed on MTB17, the propellant on which the nitrogen-rich formulations are based.

As previously reported for SB [16], some nitrogen was found by EDS on SB samples, but not consistently across reacted surfaces like in the case of MTB15 and MTB16. The presence of nitrogen associated with SB may be a result of its flame temperature compared other two propellants which may favor diffusion of nitrogen in the steel to some extent.

The effects of the presence of nitrogen-rich materials in the propellant are clearly visible in the erosion results and the composition analysis of the test pieces. It can be concluded that nitrogen-rich propellant formulations are an effective way to combat erosion and the claims that nitrogen-rich materials promote the nitriding of steel are indeed verified. The presence of nitrogen in the steel observed using

the EDS detector and the reduction in erosion of MTB15 and MTB16 demonstrate the protective effects of nitrogen well.

2.3 Performance

The addition of either BTA or HBT to the baseline formulation (MTB1&2 and MTB17) resulted in a significant increase in the burning rate of the propellant. Comparing the grains of the same geometry at 100 MPa showed a burning rate increase of 1.5 times for MTB16 and 2.4 times the burning rate for MTB15. The combined data of MTB17 and MTB1&2 was used to calculate the burning rate law parameters of the baseline formulation. Figure 16 presents the burning rates of all 5 propellants used in this work. The calculated burning rate law parameters for all propellants are presented in Table 5 with the burning rates of the SB and JAM presented for comparison.

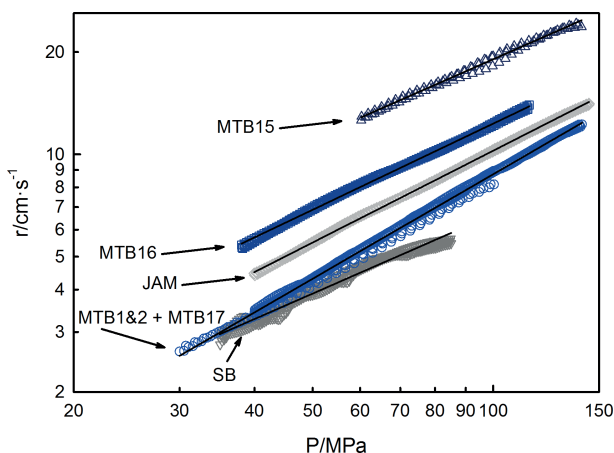


Figure 16. Burning rates of the propellants.

Table 5. Burning rate law parameters.

Propellant	$\beta/\text{cm s}^{-1}\text{-MPa}$	α	Range/MPa
SB	0.190 ± 0.010	0.772 ± 0.014	35–85
JAM	0.164 ± 0.002	0.898 ± 0.002	40–145
MTB1&2 + MTB17	0.079 ± 0.001	1.022 ± 0.004	(30–100) + (40–140) ^a
MTB15	0.532 ± 0.033	0.777 ± 0.014	60–140
MTB16	0.255 ± 0.005	0.842 ± 0.004	40–115

^aThe first range is for the MTB1&2-1 data and the second range is for the MTB17 data. The burning rate law parameters were calculated using the data from both propellants.

In addition to the increased burning rates, there is also a significant change in the linear burn rate coefficients and pressure exponents. This is different from the previously re-

ported burning rate law parameters for propellants containing BTA and HBT where an increase in pressure exponent was observed rather than a decrease [14]. This agrees with the statement that mixtures of nitrogen-rich materials with other energetics can show an increase in pressure exponent and a decrease in linear burn rate coefficient followed by the reverse when the nitrogen-rich content increases. The same type of phenomena was also observed for RDX and triaminoguanidinium azotetrazolate mixtures [13].

Internal ballistic simulations were conducted using IBGHV2 software for three particular test cases using large caliber gun. The gun parameters were determined from experimental data so that the simulated results would match them. The simulated muzzle velocity with the SB propellant was within 10% available experimental data. The first test case was where the propellants were used with their current geometries and the propellant weight charge was adjusted to match the muzzle velocity provided by SB. Case 2 is a geometry optimization of case one to fit, as much as possible, the simulated pressure curve generated by SB propellant. The third test case is where the charge weight was set to the maximum allowable by the size of the simulated gun and the pressure was limited to one serviceable by the gun to see how much the muzzle velocity could be improved with the maximum propellant charge. The grain geometry was varied to achieve the maximum serviceable pressure. The results are presented in Table 6. All results are presented relative to the simulation of the experimental data for the SB propellant.

Table 6. Ballistic performance.

Propellant	Case 1 mprop, rel	Case 2 mprop, rel	Case 3 vm, rel
SB	1.00	1.00	1.00
JAM	0.66	0.58	1.26
MTB17	0.94	0.76	1.12
MTB15	0.79	0.96	1.05
MTB16	0.84	0.80	1.13

MTB15 and MTB16 require less propellant to obtain the same muzzle velocity. MTB16 has higher energetic content, so this is expected, but MTB15 has an effectively equal energy content to SB and achieves the same performance with less propellant. This can essentially be explained by its different burn rate as the geometry of the grains is very similar to that of SB. Case 2 was chosen to demonstrate that geometry optimization would yield satisfactory performance at lower charge weight and also insure that the pressure-distance profile in the gun system remained within the operating parameters of. This was indeed the case and demonstrates that it is possible to decrease the propellant charge for a higher performance formulation without having to sacrifice the lifespan of the gun system by using a conventional high-performance, high erosivity propellant

formulation such as MTB17 or JAM. Test case 3 also illustrates that it is possible to increase performance with the maximum allowable propellant charge and to reduce erosivity altogether. It is particularly interesting that the performance of MTB16 equals that of MTB17 which is a hotter and more erosive propellant in both test cases. BTA is a very promising nitrogen-rich material for use in gun propellants. JAM was designed to match the performance of JA2 as much as possible. JA2 is a propellant currently used in high performance applications, this explains the higher muzzle velocity compared to the other high energy propellants.

3 Conclusion

The addition of nitrogen-rich materials decreases the erosivity of gun propellant formulations. The effects of nitrogen-rich materials are important enough to yield hotter propellants that are less erosive than conventional ones. Part of the reduction in the erosivity is due to nitrogen diffusion in and reacting with the steel compared to the reference conventional propellant. The higher nitrogen content limits, but does not prevent the formation of carbides and oxides resulting from the presence of CO and CO₂. The addition of nitrogen-rich materials had a significant impact on the burning rate of the reference propellant with significantly higher burning rates and lower pressure dependency. The increased burning rates had an effect on the erosivity results for the fastest burning propellants due to higher velocity gas flow. The simulated ballistic performance of the nitrogen-rich propellants was as good as the initial test case or better.

4 Experimental Section

The nitrogen-rich materials used in this work were synthesized at the General Dynamics Ordnance and Tactical Systems (GD-OTS) Valleyfield facilities in kilogram batches using a 30 L glass reactor. The facilities available at GD-OTS Valleyfield allowed for the safe scale-up of energetic materials. 5,5'-bis (1H-tetrazolyl) amine (BTA) was synthesized according to the experimental protocol already described in the literature [17] and was performed with ease. The synthesis of 5,5'-hydrazinebistetrazole (HBT) was modified from the original protocol [18] due to issues appearing during the scale-up operations. The purity of the materials was assessed using ¹H NMR and ¹³C NMR, no impurities were detected.

Five propellants were used in this work: a standard simple base propellant (SB), a modified JA2 triple-base propellant (designated JAM), the same reference triple-base used in a previous work (MTB17) [14] and two propellants each incorporating one nitrogen-rich crystal at 35% weight concentration, either BTA (MTB16) or HBT (MTB15). Table 7 shows the composition of the propellants.

Table 7. Propellant constituents.

Propellant	Constituents
SB	NC (13.4%N); DNT; DBP; DPA
MTB15	NC (13.25%N); TMETN; TEGDN; HBT; EC
JAM	NC (13%N); NG; TEGDN; AK II
MTB16	NC (13.25%N); TMETN; TEGDN; BTA; EC
MTB17	NC (13.25%N); TMETN; TEGDN; EC

JAM is a good benchmark for erosivity as it is a very hot propellant, generally known for being highly erosive. JAM propellant was designed to match the thermochemical properties the propellant incorporating BTA (MTB16) and was manufactured at the GD-OTS Valleyfield pilot plant. SB was also provided by GD-OTS Valleyfield. Finally, the two propellants incorporating nitrogen-rich materials were manufactured using the facilities available at DRDC-Valcartier in a 1 USG (3.7 L) Bayer-Perkins sigma blade mixer, as described previously [13, 14]. All propellants were extruded to a cylindrical 7 perforations geometry. MTB15 was extruded to have 7 perforations cylindrical geometry equivalent to that of SB. MTB16, MTB17 and JAM were extruded using a larger 7 perforations cylindrical geometry.

The pressure-time data used in the determination of the burning rates was acquired using a RARDE closed vessel, model CV21, V = 700 cm³. An internal sleeve was used to reduce the volume of the closed vessel to approximately 180 cm³. The exact volume was measured prior to each test. All propellants were fired at a loading density of 0.2 g cm⁻³. 1 g of black powder was used to achieve ignition of the propellant. The burning rate data for each closed vessel firing was calculated using the XLCB software. Burning rate law parameters were calculated by performing regression on the logarithm form of Vielle's law. The pressure range to which the regressions were applied was chosen by analysis of the dynamic vivacity curves. The use of vivacity to validate the data range over which regressions can be performed has previously been discussed [19, 20].

The erosivity was measured using a vented vessel of custom design. The erosion pieces were made of 4340 AISI steel and had an initial opening diameter of 1 mm. The vessel was not equipped with a rupture disc; hence the combustion gases were free to escape the vented vessel as soon as combustion of the propellant occurred. A diagram of the vessel is presented in Figure 17.

In order to assess the cumulative effects of combustion gases on the same erosion piece, each propellant was fired 1 to 3 times per erosion piece. Scanning electron microscopy (SEM) coupled with energy dispersive X-ray spectroscopy (EDS) was performed using a JEOL JSM-7600TFE scanning electron microscope equipped with an Oxford Instruments EDS detector. Erosion pieces were cut in half prior to SEM-EDS experiments. An analysis of an erosion piece that was not submitted to testing was used as the baseline for carbon contamination from handling and or-

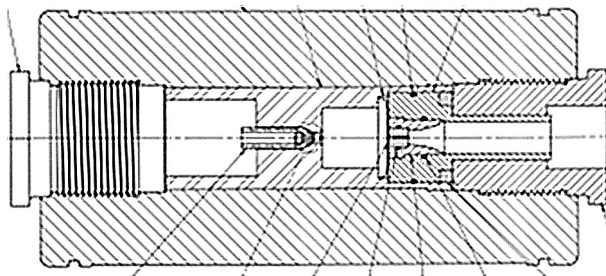


Figure 17. Vented vessel apparatus.

ganics. It was also used to determine if cutting resulting in the presence of impurities. Each erosion piece was washed with acetone, hexanes and methanol using both an ultrasonic bath and cotton swabs. The SEM measurements were taken in the channel where contact between the combustion gases and the steel occurred.

The ballistic performance was calculated with the IBHVG2 software. The software was calibrated using experimental data for the simulated gun prior to performing any simulations on the experimental propellants.

Acknowledgements

The authors would like to acknowledge the contributions of Étienne Comtois, Simon Durand, Véronique Parent and Alain Gagnon who made the scaling-up of the syntheses possible. Thanks to Dr. Daniel Chamberland from DRDC who provided the purity assessment tby NMR and to Charles Nicole and Pascal Béland for performing the vented vessel and closed vessel experiments.

References

- [1] P. J. Conroy, C. S. Leveritt, J. K. Hirvonen, J. D. Demaree, *The Role of Nitrogen in Gun Tube Wear and Erosion*, U.S. Army Research Laboratory, Aberdeen Proving Ground, MD ARL-TR-3795, 2006.
- [2] P. J. Conroy, P. Weinacht, M. J. Nusca, *Gun Tube Coatings in Distress*, U.S. Army Research Laboratory, Aberdeen Proving Ground, MD ARL-TR-2393, 2001.
- [3] S. Sopok, C. Rickard, S. Dunn, Thermal-chemical-mechanical gun bore erosion of an advanced artillery system part one: theories and mechanisms, *Wear*, **2005**, 258, 659–70.
- [4] B. Lawton, Thermo-chemical erosion in gun barrels, *Wear*, **2001**, 251, 827–838.
- [5] I. A. Johnston, *Understanding and Predicting Gun Barrel Erosion*, Weapons Systems Division - Defence Science and Technology Organisation 2005.
- [6] Published by the Organizing Committee – B. Lawton, Thermal and Chemical Effects of Gun Barrel Wear, Proceedings of the 21st International Symposium on Ballistics, Adelaide, Australia, 2004 .
- [7] S. Jaramaz, D. Mickovic, P. Elek, Determination of gun propellants erosivity: Experimental and theoretical studies, *Exp. Therm. Fluid Sci.*, **2010**, 34, 760–765.
- [8] P. J. Cote, C. Rickard, Gas-metal reaction products in the erosion of chromium-plated gun bores, *Wear*, **2000**, 241, 17–25.
- [9] Published by American Defense Preparedness Association, J. Kimura, Hydrogen Gas Erosion of High-Energy LOVA Propellants, 16th International Symposium on Ballistics, San Francisco, CA, USA, 1996.
- [10] P. J. Conroy, J. S. Montgomery, L.-S. Lussier, F. Beaupré, B. Jones, TTCP WPN/TP4 KTA 4–26 Gun Tube Wear and Erosion Final Report, U. S. Army Research Laboratory, Aberdeen Proving Ground, MD, ARL-TR-2935, 2003.
- [11] T. M. Klapötke, *Chemistry of High-Energy Materials*, 2 ed., De Gruyter, Berlin 2012.
- [12] N. Fischer, D. Izsak, T. M. Klapotke, S. Rappenglück, J. Stierstorfer, Nitrogen-rich 5,5-bistetrazolates and their potential use in propellant systems: A comprehensive study, *Chem. Eur. J.*, **2012**, 18, 4051–4062.
- [13] B. A. Mason, J. M. Lloyd, S. F. Son, B. C. Tappan, Burning rate studies of bis-triaminoguanidinium azotetrazolate (TAGzT) and hexahydro-1,3, 5-trinitro-1, 3, 5-triazene (RDX) mixtures, *Int. J. Energ. Mater. Chem. Propul.*, **2009**, 8, 31–38.
- [14] J. Lavoie, C.-F. Petre, P.-Y. Paradis, C. Dubois, Burning Rates and Thermal Behavior of Bistetrazole Containing Gun Propellants, *Propellants Explos. Pyrotech.*, **2017**, 42, 149–157.
- [15] R. E. Kaczmarek, M. S. Firebaugh, B. M. Rice, T. M. Klapötke, J. M. Short, R. D. Lynch, *Topics in Energetics Research and Development*, ESPC Press, 2013.
- [16] W. T. Ebihara, D. Rorabaugh, T., Mechanisms of Gun-Tube Erosion and Wear, *Progress in Astronautics and Aeronautics* vol. 109, Washington DC, United States: AIAA, 1988.
- [17] T. M. Klapotke, P. Mayer, J. Stierstorfer, J. J. Weigand, Bistetrazolylamines-synthesis and characterization, *J. Mater. Chem.*, **2008**, 18, 5248–5258.
- [18] T. M. Klapotke C. M. Sabate, Bistetrazoles: nitrogen-rich, high-performing, insensitive energetic compounds, *Chem. Mater.*, **2008**, 20, 67–75.
- [19] Published by Johns Hopkins University, K. W. Klingaman J. K. Domen, The Role of Vivacity in Closed Vessel Analysis, JANNAF Propellant Development and Characterization Subcommittee Meeting, Patrick AFB, FL, USA, 1994.
- [20] W. F. Oberle, Dynamic vivacity and Its Application to Conventional and Electrothermal-Chemical (ETC) Closed Chamber Results, U. S. Army Research Laboratory, Aberdeen Proving Ground, MD, USA, 2001.

Received: November 6, 2017

Accepted: April 30, 2018

Published online: August 30, 2018